Interface roughening dynamics: Temporal width fluctuations and the correlation length

Avraham Be'er, Inbal Hecht, and Haim Taitelbaum
Department of Physics, Bar-Ilan University, Ramat-Gan 52900, Israel
(Received 8 November 2004; published 22 September 2005)

In this work we study experimentally and numerically the temporal width fluctuations obtained in kinetic roughening of single interfaces. This fluctuative behavior, which results from competing mechanisms in the interface growth process, is shown to contain information on the growth process of the specific interface. We define a measure of the temporal interface width fluctuations in order to extract the correlation length of the interface from the fluctuating data. We study numerically the quenched Kardar-Parisi-Zhang (QKPZ) equation for single interfaces in order to assess the role of the different mechanisms, such as normal growth and surface tension, on the fluctuations. We analyze experimental data of mercury droplets spreading on various metal films (silver and gold) in various thicknesses, as well as data of water spreading on paper (imbibition), in order to demonstrate the validity of our method in a wide range of growing interfaces.

DOI: 10.1103/PhysRevE.72.031606 PACS number(s): 68.08.Bc, 68.37.−d, 89.75.Da

I. INTRODUCTION

During the past decades, many scientists of different disciplines were extensively investigating the dynamics and geometry of growing interfaces using the concepts of self-affine and fractal scaling [1–28]. Among the possible applications of kinetic interfacial roughening one can mention processes such as imbibition, wetting, burning, and fracture [6]. In this paper, we study the spatiotemporal dynamics of a growing interface, following a series of experimental studies of spreading mercury droplets on thin metallic films [26–28]. Such spreading processes are of great interest and importance in material science, optics and technology, with a diverse range of applications, e.g., soldering, typing and painting, gluing, condensation of droplets on solid substrates, and coating of glasses by photoresist liquids in photolithography processes [29–36].

Droplet spreading on metallic films is very complicated [29–31]. It involves the motion of a contact line due to hydrodynamic forces as well as a chemical reaction between the mercury and the solid metal. In a different publication [32] we have recently addressed another aspect of this complicated phenomenon, which is the dynamic *three*-dimensional shape of the spreading droplet, as obtained by the optical microscope in a newly developed, time-resolved, technique. However, in this paper we focus on the *interface characteristics* (roughness and growth) of the spreading phenomenon, as observed by a microscope top view. These characteristics are expected to capture the essential physical features of the entire system [6], and have not been studied earlier for spreading droplets.

A possible theoretical treatment of a propagating self-affine interface is based on constructing a continuum differential equation for describing the motion of the interface. The simplest nonlinear Langevin equation for a local interface growth is the Kardar-Parisi-Zhang (KPZ) [7] equation:

$$\frac{\partial h}{\partial t} = \nu \nabla^2 h + \frac{\lambda}{2}(\nabla h)^2 + \eta(x,t), \tag{1}$$

where $h(x,t)$ is the interface height at position x at time t, ν is the surface tension, λ is proportional to the velocity normal to the interface and η is a noise term. A possible variant of the KPZ equation is QKPZ (Quenched disorder KPZ) [4,5], which assumes that the noise term depends on the spatial coordinates rather than the time, i.e., $\eta(x,h)$ instead of $\eta(x,t)$. Analysis of these equations under certain conditions can predict sets of scaling exponents [8]. In particular, the width W of the interface, which is formally defined as

$$W^2(L,t) = \langle h(x,t)^2 \rangle - \langle h(x,t) \rangle^2, \tag{2}$$

has been assumed to obey a power law in time t and distance L, with two scaling exponents, α, the roughness exponent and β, the growth exponent, defined as

$$W \sim \begin{cases} t^{\beta}, & t \ll t_0, \\ L^{\alpha}, & t \gg t_0, \end{cases} \tag{3}$$

where $t_0 \approx L^{\alpha/\beta}$, and L is a window varying from the smallest length scale (say a single lattice unit) to the system size L_0.

Although many theoretical studies [1–11] (analytical, numerical, or simulations of discrete models) study both the roughness and the growth exponents, only a few experimental works were able to measure the growth exponent β [12–22,26–28]. While the roughness exponent α was measured or calculated in order to study properties of the system, such as the characteristic correlation length of the interface, the growth exponent β was mainly studied in order to complete the classification of the system, together with the roughness exponent α, into a specific universality class. Examples of such universality classes are $\alpha+\alpha/\beta=2$ in isotropic systems [8,12,26–28], $\alpha/\beta=4$ in the surface diffusion universality class [4], $\alpha=\beta$ in some pinned systems [23] and also $\alpha+\alpha/\beta=4$ [24] and $\alpha/\beta=2$ [25].

Among the few works that did calculate the growth exponent β [12–22,26–28], only very few presented actual pictures of interface lines and their time evolution [12,13,15,18–20,27]. Most of these studies referred to a finite number of growing interfaces, sometimes a single interface only. It was shown that one can describe the interface width as growing monotonically with time, obeying a standard power-law behavior with an exponent β [15–20,26–28]. However, a closer look at these results shows that there exist

 ©2005 The American Physical Society

fluctuations in the log-log plots of W as a function of time. This was pointed out by Balankin *et al.* [21] who performed paper-wetting experiments, as well as by Soriano *et al.* [22] who measured interfacial roughening in Hele-Shaw flows. They attributed the strong temporal fluctuations in $W(t)$ to the details of the disorder configuration in their experimental systems, and commented that the fluctuations should be smoothed out when more samples are averaged.

In this paper we show, experimentally and theoretically, that this behavior always emerges when a finite number of interfaces is involved, as may be the case, e.g., in experiments or industrial applications. By studying the KPZ equation we show that this unique feature of the dynamical growth results from the competition between the two mechanisms: the *normal growth*, which tends to *roughen* the interface, and the *surface tension forces*, which tend to *smooth* it. This competition averages out when an infinite number of interfaces is taken into account. However, for given interfaces, in particular for single interfaces, these fluctuations contain hidden information on the specific system and its growth characteristics, in particular the *correlation length*.

For many interface growth processes there exists a typical length scale of which below and above it different mechanisms govern the dynamics and growth of the interface. This length, also known as the correlation length [1–5,11], or, similarly, the lateral length scale [6], represents the length scale of collective growth of the interface. The growth of portions of the interface above this length is not correlated. An estimation of the correlation length is usually obtained using the roughness properties of the interface. The roughness exponent α is related to the height-difference correlation function on the interface [1],

$$C(L) = [\langle (h(x) - h(x'))^2 \rangle_x]^{1/2} \sim L^{\alpha}, \tag{4}$$

where $|x-x'|=L$. Values of $0.5<\alpha<1$ represent correlated motion, while values of $\alpha \sim 0.5$ represent a random, non-correlated motion (e.g., random walk) [1–5]. In other words, this length fixes the maximum range of correlated roughness [6]. Therefore, the correlation length is a crossover point between $\alpha > 0.5$ and $\alpha \leqslant 0.5$ in the $W(L)$ plots [Eq. (3)]. In the following we show how to extract the correlation length from the experimental data in much earlier stages of the interface growth process, based on the temporal growth fluctuations.

The paper is organized as follows. In Sec. II we present the experimental setup and describe in detail the data analysis procedure from which we extract the correlation length. In Sec. III we study numerically the QKPZ equations and show the effect of the nonlinear growth and the surface tension parameters on the size of the fluctuations. We also show how the fluctuations vanish when more realizations are taken into account. In Sec. IV we show data analysis of other experimental systems where significant experimental parameters, such as the film thickness and type, are changed. In Sec. V we apply our method to other experimental data in the literature (water imbibition in paper) in diverse time and length scales. This allows us to summarize, in Sec. VI, the generality of our approach.

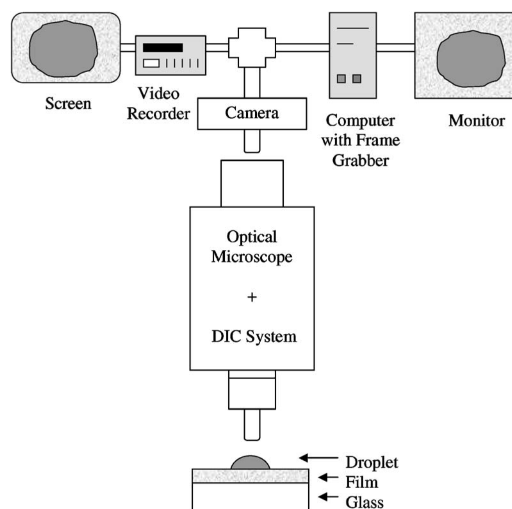

FIG. 1. A schematic view of the experimental system.

II. EXPERIMENTAL RESULTS AND DATA ANALYSIS

The experimental system is shown in Fig. 1. Silver (Ag) films were either deposited on glass microscope slides by vacuum evaporation (thickness range 2000–4000 Å), or were polished by diamond powder (thickness 0.1 mm). Gold (Au) thin films (1500 Å) were produced as well using the vacuum evaporation technique. Small droplets of mercury (Hg) (150 μm in diameter) were placed on these metal substrate surfaces. The spreading process of the Hg droplet on the metal surfaces has been monitored using an optical microscope equipped with a differential interference contrast (DIC) system. The Hg front propagation has been recorded by a video camera. The duration of the experiments was several minutes. The images were analyzed in order to determine the geometrical and dynamical properties of the front, according to Eq. (3). The results for the roughness and growth exponents of the spreading process on thin Ag films have been reported in [26,27], while the corresponding results for spreading on Au films can be found in [28].

In order to calculate the dynamical growth properties of the interface width, according to Eq. (3), one has to pick an arbitrary window size L along the interface line. This window is used repeatedly until the entire interface is covered. The height of the interface in each window is measured, and the width of the interface is finally obtained as the average height of all these heights. This procedure is repeated for the growing interface at every time t. In Fig. 2 we show typical results for $W(t)$ for two different single processes. In Fig. 2(a) the metal film thickness is 2000 Å, whereas in Fig. 2(b) the film thickness is 0.1 mm. In both cases one can fit a straight line in order to obtain the single-interface growth exponent β, but the fluctuations are evident and cannot be ignored. This fit has been found to be robust with respect to these fluctuations, and independent of the chosen window size. In Fig. 3(a) we replot the results of Fig. 2(b) for 8 different window sizes L, ranging from 3 to 25 μm (10 to 80 pixels). As can be seen, the single-interface growth

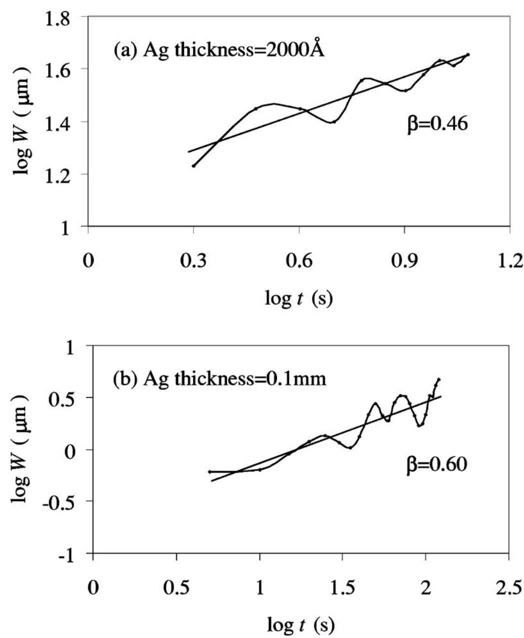

FIG. 2. The function $W(t)$ calculated from a single experiment's data in the Hg-Ag system. (a) Ag thickness is 2000 Å and window size L is 10 μm. (b) Ag thickness is 0.1 mm and window size L is 18 μm. Both log-log plots show a nonmonotonic function riding over a straight line. The slope of this line is the growth exponent β whose values are indicated.

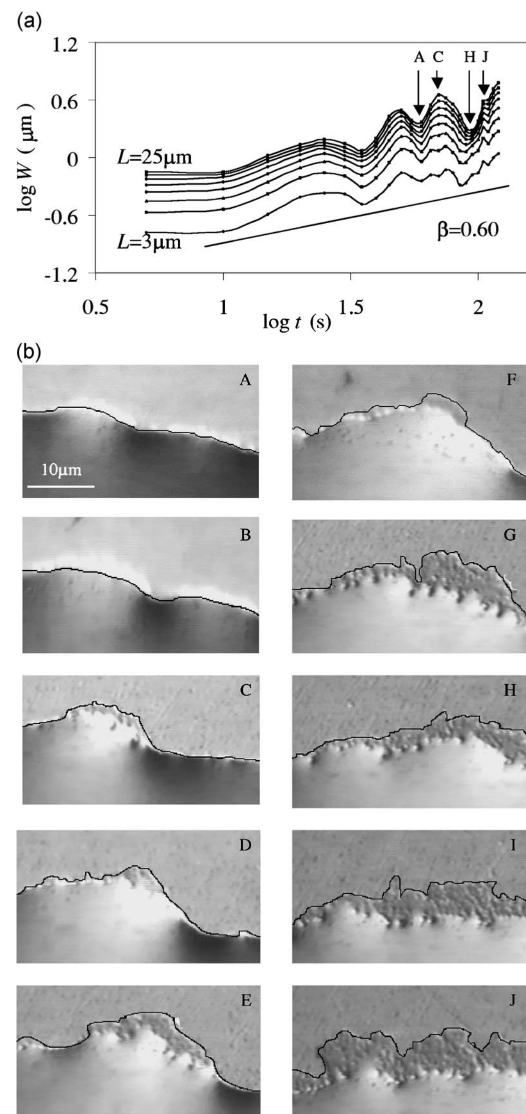

FIG. 3. (a) The function $W(t)$ in the thicker Hg-Ag system [Ag thickness 0.1 mm as in Fig. 2(b)] for several window sizes L, varying from 3 to 25 μm (10 to 80 pixels). All slopes are approximately equal to 0.60. Chosen points on the graph, belonging to extreme points, are marked by A, C, H, J. (b) A series of successive snapshots taken at times 60–105 s with intervals of 5 s. We mark these snapshots by A–J, which correspond to the times A–J indicated in (a). The total horizontal size is 35 μm (110 pixels). One can clearly see the local increase of the interface width in times C, and the local decrease of the width around H, followed by another increase in J.

exponent β is independent of the window size L. Moreover, the fluctuations occurrence times are also independent on L. This implies that the fluctuations reflect an intrinsic property of this single system.

It should be emphasized that fitting a straight line to the fluctuative data of a single interface stems from the scaling law given in Eq. (3), which is expected to be valid for the *sample-averaged* width W [21,22]. The slope of the straight line when a *single interface* is concerned should be regarded as a *single-interface* growth exponent.

In order to gain insight on the origin of the systematic temporal fluctuations, one should check the temporal history of the interface growth process. In Fig. 3(b) we follow, in a series of successive snapshots, a few stages in this process in a given interface portion of total size $L_0=35$ μm (110 pixels). We mark these snapshots, taken at times 60–105 s with intervals of 5 s, by A–J. Snapshots A, C, H, J correspond to the times indicated on Fig. 3(a). One can clearly see the local increase of the interface width in time C, with respect to time A, and the local decrease of the width around H, followed by another increase in J.

The specific shape of these fluctuations varies from sample to sample. Thus, these sample-dependent fluctuations must contain hidden physical characteristics of the specific system under consideration. In order to extract this information we define a new measure of the width fluctuations, based on the difference between successive minima and maxima in the log-log plot of the width W vs the time t. Formally, this measure, $\Delta \log W$, will be defined as

$$\Delta \log W = \frac{\sum_{i=j} |M^y{}_i - m^y{}_j|}{i}, \qquad (5)$$

where $M_i{}'s$ are local maxima and $m_j{}'s$ are local minima in the plot of log W vs log t (Fig. 2). We take $i=j$ in order to get the "peak to peak" deviations from the straight line. Next, if we plot this measure $\Delta \log W$, as a function of the window size L [Fig. 4(a)], it can be seen that the larger is L, the larger are the fluctuations $\Delta \log W$. This is intuitively clear, since

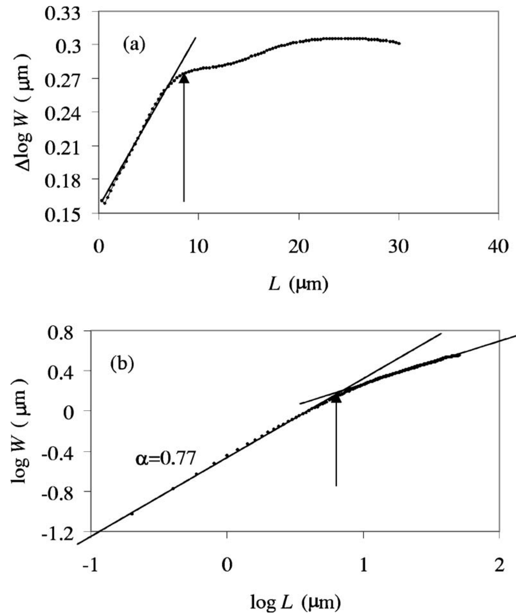

FIG. 4. (a) The measure of the width fluctuations $\Delta \log W$ [Eq. (5)] as a function of the window size L. A crossover is marked with an arrow for $L=8.1\ \mu\text{m}$ (27 pixels). (b) The roughness exponent α, as obtained from the log-log plot of $W(L)$ at the end of the experiment. The crossover occurs at the same characteristic length $L=8.1\ \mu\text{m}$ (27 pixels) as in (a). The roughness exponent was found to be $\alpha=0.77$ below the crossover.

smaller windows can only reflect smaller, local fluctuations. Moreover, the plot of $\Delta \log W$ vs L reveals a crossover behavior below and above a characteristic value of the window size L. A linear trend line is fitted to the data of the plot of $\Delta \log W$ vs L, starting at the smaller L's [see Fig. 4(a)]. We define the crossover point, L_β, as the point in which the square of the sample-correlation-function of the linear fit, denoted by R^2 [37], becomes smaller than 0.99. In the particular system shown in Fig. 4(a), this characteristic value is about 8.1 μm (27 pixels).

In general, when the spreading process ends, the function $W(L)$ (the graph of the roughness exponent α) exhibits a crossover behavior at some window size L_α [Fig. 4(b)] (see, e.g., [12]). This typical window size, L_α is the correlation length of the interface, of which below, points on the interface advance ahead in correlation with their neighbors. Above this point there is no correlation and thus the value of the slope (i.e., α) goes to 0.5, which, as mentioned earlier, represents a random, noncorrelated motion. Our results for the characteristic length (L_β) obtained from the width fluctuations were found to be consistent with this correlation length (L_α), obtained from the roughness exponent crossover behavior. This means that this typical length can be obtained at much earlier stages of the process, through the fluctuations in the time-dependent growth function.

It is interesting to note that Fig. 4(b) indicates that $W(L)$ is perfectly smooth, even for a single interface, unlike the behavior of $W(t)$. Experimental data of $W(L)$ in the literature [3,17–20,26,28,38,39] also indicate a smooth function from which one obtains the roughness exponent α. The difference between $W(L)$ and $W(t)$ results from the fact that $W(L)$ is plotted for a given time, and does not describe a dynamic quantity. Thus the fluctuative behavior of $W(t)$ is a unique characteristic of the dynamically growing interface.

III. QKPZ EQUATION: NUMERICAL CALCULATIONS

What is the physical interpretation of such a fluctuative behavior? In order to answer this question we solved the QKPZ equation numerically for a single interface. This version of the KPZ equation resembles our experimental system in the sense that surface film defects induce time-independent quenched noise into the system [27]. It should be emphasized that the relatively simple description of the QKPZ equation cannot fully describe our complicated system [6]. However, comparing our results with the QKPZ interface dynamics will allow us to gain insight on the basic physics behind such temporal fluctuations.

Our numerical system consisted of a $(1+1)$-dimensional interface of 500 points (pixels), initially flat. Each point in the lattice was initialized with a random noise value, chosen from a distribution with zero mean. Both Gaussian and uniform distributions were used. We have then solved numerically the QKPZ equation for this system [Eq. (1) with quenched noise]. We used the forward time centered space (FTCS) scheme [40] for the numerical integration with time intervals of $\Delta t=0.1$ and $\Delta t=0.05$, for a wide range of the parameters set (λ, ν). Interface characteristics were calculated using the method described above.

In Fig. 5(a) we show the result for the width W as a function of time t, for a solution of Eq. (1) for a single interface, with $\lambda=0.1$, $\nu=0.15$ and uniformly distributed quenched noise in the range $(-1,1)$. The fluctuations patterns are similar to those obtained in the corresponding experimental plots in Figs. 2 and 3(a). From the existence of such fluctuations in the relatively simple case of the QKPZ equation, we infer that the nonmonotonic growth of the width $W(t)$ is a fundamental feature of interface roughening dynamics. It results from the competing mechanisms in the growth process, i.e., the nonlinear growth (represented by λ) and the surface tension (ν).

When a local gradient in the interface height occurs, due to the noise, a hump in the interface is created. Then the nonlinear term tends to increase its size, whereas the surface tension tends to decrease it. The result of this competition is the local growth fluctuations, which are reflected in the overall temporal behavior of the width W as a function of time. It should be noted that the surface tension mechanism is acting in a "time delay" relative to the nonlinear growth, because it responds to the growth after it has happened, and this is the reason for the nonmonotonic behavior: advance due to the nonlinear term, and then regression due to the surface tension.

In Fig. 5(b) we show the plot of $\Delta \log W$ [the fluctuations measure, as was defined in Eq. (5)] as a function of the window size L, from which one can obtain the correlation length (in this system $L\approx 70$ pixels). As in the experimental case, this value is verified by the crossover in the plot of W as a function of L [Fig. 5(c)] at the end of the interface growth process, which also occurs around $L\approx 70$ pixels.

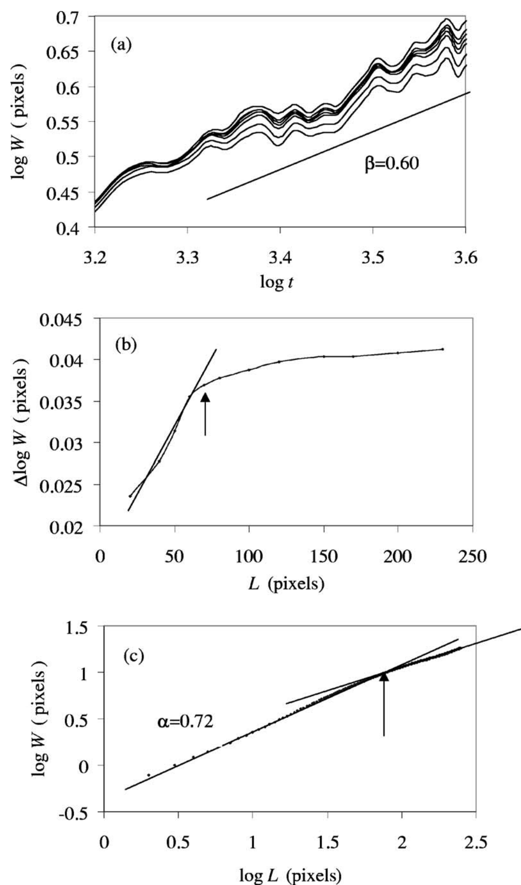

FIG. 5. (a) A log-log plot of the width W as a function of t, obtained from the numerical solution of the QKPZ equation for a single interface in the FTCS method, with $\lambda=0.1$, $\nu=0.15$, for various window sizes $L=70,80,100,120,150,200,230$ pixels, represented by the different lines (from bottom to top). The nonmonotonic function over the straight line $\beta=0.60$ resembles the experimental curves in Fig. 3(a). (b) The measure of the width fluctuations $\Delta \log W$ as a function of the window size L, as obtained from the data in (a). A crossover is marked with an arrow for $L=70$ pixels. (c) A log-log plot of the width W as a function of the window size L. The slopes represent the values of the roughness exponent α, below and above the same crossover length $L=70$ pixels as in (b). The roughness exponent was found to be $\alpha=0.72$ below the crossover.

This behavior is typical for a single interface with a given set of the parameters (λ,ν). In order to study a wide range of the parameter space, we performed extensive data analysis. In these calculations, a slightly different method was used for the fluctuations size measure. We calculated the linear fit for the nonmonotonic graph of $\log W$ vs $\log t$, and the deviations from the straight line. We averaged the square of these deviations over the time series and obtained the characteristic value ϕ, defined as

$$\phi = \sqrt{\langle(\log w_i - \log w_i^{linear})^2\rangle_i}, \tag{6}$$

where w_i is the width of the interface at time i, and $\log w_i^{linear}$ is the value of the linear fit for time i. The brackets denote average over time.

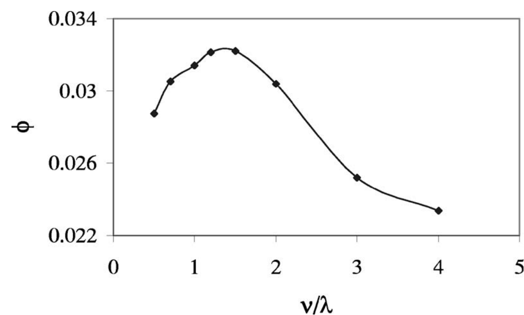

FIG. 6. The fluctuations size ϕ [defined in Eq. (6)] as a function of the ratio of the parameters ν,λ. The fluctuations size is maximal when $\nu\sim\lambda$.

We studied different sets of parameters (λ,ν) and two different noise distributions (uniform and Gaussian). We measured the correlation length from the early-time fluctuations as well as from the roughness exponent behavior at long times, and in all cases these two measures were consistent, similarly to the findings presented in Fig. 5. However, we found that the values of the parameters λ,ν do influence the *size* of the fluctuations. In Fig. 6 we show that the fluctuations size ϕ [Eq. (6)] exhibits a noticeable maximum when $\nu\sim\lambda$, namely, when the two opposing mechanisms are of the same order of magnitude. This supports the argument that the interface width fluctuations are due to this competition.

It is clear that the particular correlation length provides an estimate for the average correlation length in all the similar interfaces produced under similar conditions. It also allows

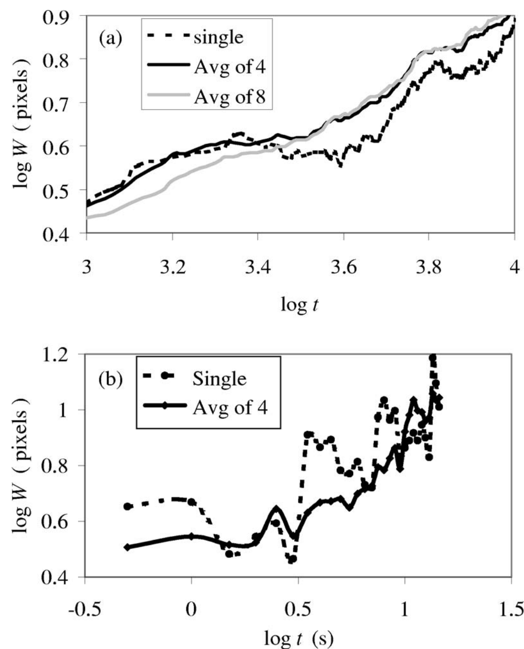

FIG. 7. (a) Numerical data for the width as a function of time (in a log-log scale), with $\nu=0.1$, $\lambda=0.1$, and $L=160$ pixels, for (i) a single interface; (ii) the average of 4 interfaces, and (iii) the average of 8 interfaces. (b) Experimental data of the 2000 Å Ag system with $L=50$ pixels (3 μm): The width as a function of time (in a log-log scale), for (i) a single interface and (ii) the average of 4 interfaces.

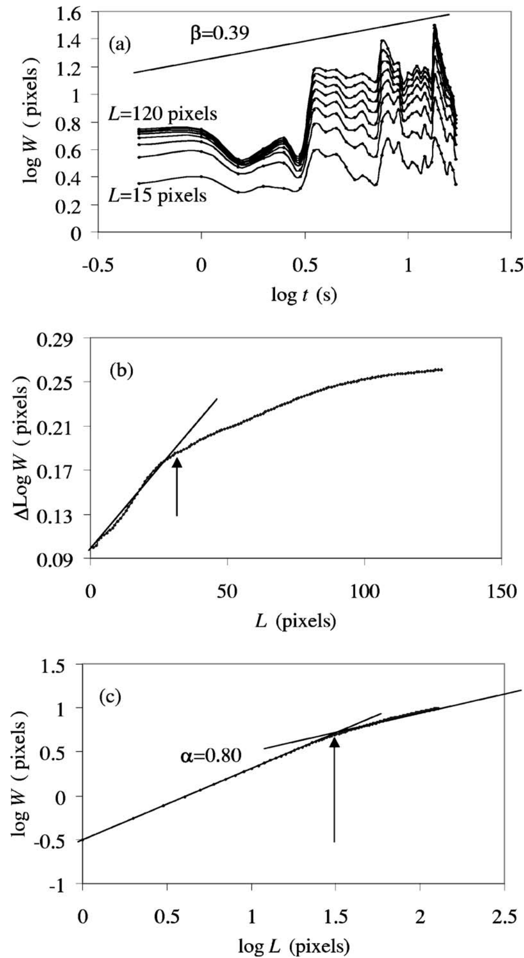

FIG. 8. (a) The function $W(t)$ in the 2000 Å Hg-Ag system for several window sizes L, varying from 15 to 120 pixels, which are about 1 to 7.5 μm. All slopes are approximately equal to 0.39. (b) The measure of the width fluctuations $\Delta \log W$ [Eq. (5)] as a function of the window size L. A crossover is marked with an arrow for $L=32$ pixels (1.9 μm). (c) The roughness exponent α, as obtained from the log-log plot of $W(L)$ at the end of the experiment. The crossover occurs at almost the same characteristic length $L=28$ pixels (1.7 μm) as in (b). The roughness exponent was found to be $\alpha=0.80$ below the crossover.

one to provide an estimate of the sample-averaged growth exponent β. The numerical calculations allow us to perform multiple runs, in order to get a better sense of the run-to-run divergence. In Fig. 7(a) we show what happens when more realizations of single interface growth are taken into account. In this figure the width of the interface is averaged over 4 and over 8 realizations, and it is shown that even for a small number of interfaces the fluctuations tend to vanish. The interface width behaves then according to the scaling law $W \sim t^{\beta}$, which gives the straight line in the log-log plot. The size of the fluctuations of the average interface is very small relative to the fluctuations size of a single interface and it is almost independent of L. Figure 7(b) is similar to Fig. 7(a) but for *experimental* data of the 2000 Å Ag system.

IV. MORE EXPERIMENTAL DATA

In order to substantiate the validity of our method in a wide range of growing interfaces, we have performed more experimental studies, in which we have changed some of the significant experimental parameters, such as the thickness of the metal film, or the type of the metal itself.

A. Hg-Ag system with various Ag thicknesses

The dynamics and growth of the propagating fronts, observed when small Hg droplets spread on Ag films, depend on different mechanisms [26,27]. One of these mechanisms is the chemical reaction between the droplet and the surface, which may be highly influenced by the surface's structure of the Ag layer, as well as its total thickness. For this reason we have investigated both thick Ag foils of 0.1 mm, polished by diamond powder [see Figs. 2(b), 3, and 4], as well as thinner Ag films (2000–4000 Å) produced using vacuum evaporation. These two methods yield different surface structures. In the following we refer to two different thicknesses of the thinner film category: 2000 Å and 4000 Å. In these experiments 1 pixel corresponds to about 0.061 μm (different magnitudes were used for different experiments).

In Fig. 8 we show the results of a single spreading process on a 2000 Å Ag film. As can be seen [Fig. 8(a)], the value of β is independent of L and the large fluctuations are evident. It can be seen that the crossover point obtained in the graph of $\Delta \log W$ [Fig. 8(b)] at 32 pixels (1.9 μm), is very close to the crossover point in the graph of the roughness exponent α at the end of the spreading process [Fig. 8(c)] at 28 pixels (1.7 μm). Similarly, Fig. 9 summarizes the data of a single experiment of the 4000 Å system. It can be seen that the crossover point obtained in the graph of $\Delta \log W$ [Fig. 9(b)] at 15 pixels (0.9 μm), is very close to the crossover point in the graph of the roughness exponent α at the end of the spreading process [Fig. 9(c)] at 14 pixels (0.85 μm).

We have thus shown that our method is quite accurate in estimating the correlation length of a single interface. We will next show that this correlation length can be used as the correlation length of the entire class of systems under study. For example, we have performed four different experiments for the 2000 Å Ag thickness system, one of which is shown in Fig. 8. The growth exponent for these four systems has

TABLE I. The values of the correlation lengths observed in the graph of α, L_{α}, compared to the values of the characteristic length scales observed in the graph of $\Delta \log W$ vs L, L_{β}, for four different single interfaces of the 2000 Å Ag system. All values are in μm.

No. of experiment	L_{α}	L_{β}
1	1.7	1.9
2	4.6	3.9
3	3.9	3.9
4	1.5	1.4
Average	2.9±1.3	2.8±1.1

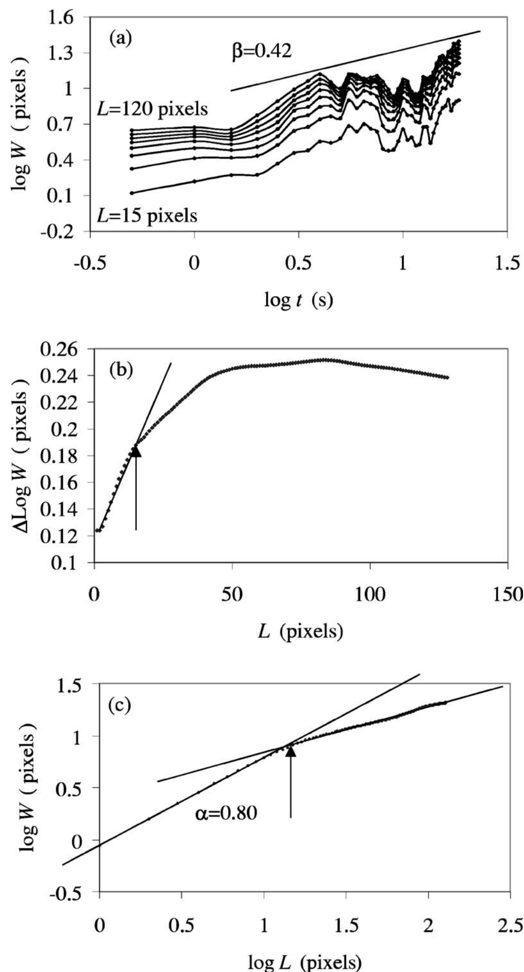

FIG. 9. (a) The function $W(t)$ in the 4000 Å Hg-Ag system for several window sizes L, varying from 15 to 120 pixels, which are about 1 to 7.5 μm. All slopes are approximately equal to 0.42. (b) The measure of the width fluctuations $\Delta \log W$ [Eq. (5)] as a function of the window size L. A crossover is marked with an arrow for $L=15$ pixels (0.9 μm). (c) The roughness exponent α, as obtained from the log-log plot of $W(L)$ at the end of the experiment. The crossover occurs at almost the same characteristic length $L=14$ pixels (0.85 μm) as in (b). The roughness exponent was found to be $\alpha=0.80$ below the crossover.

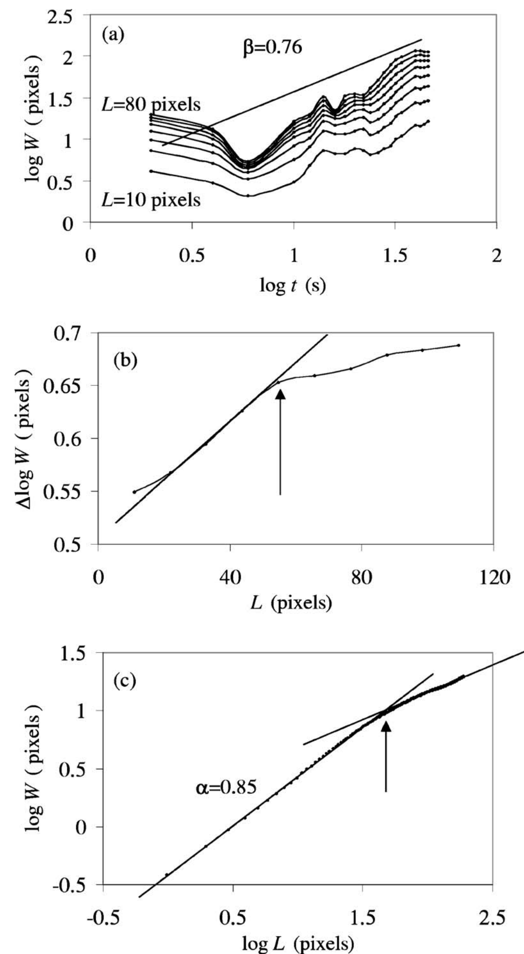

FIG. 10. (a) The function $W(t)$ in the 1500 Å Hg-Au system for several window sizes L, varying from 10 to 80 pixels which are about 1.6 to 12.8 μm. All slopes are approximately equal to 0.76. (b) The measure of the width fluctuations $\Delta \log W$ [Eq. (5)] as a function of the window size L. A crossover is marked with an arrow for $L=54$ pixels (8.5 μm). (c) The roughness exponent α, as obtained from the log-log plot of $W(L)$ at the end of the experiment. The crossover occurs approximately at the same characteristic length $L=45$ pixels (7 μm) as in (b). The roughness exponent was found to be $\alpha=0.85$ below the crossover.

been found to be $\beta=0.42\pm0.04$. Table I summarizes the results for the characteristic lengths. For each ofthe single runs the value of the correlation length taken from the graph of α is almost equal to the corresponding length scale observed in the $\Delta \log W$ vs L graph. When averaging the four cases we get $L_{\alpha}=48\pm22$ pixels (2.9±1.3 μm) and $L_{\beta}=47\pm18$ pixels (2.8±1.1 μm). The somewhat large standard deviations reveal the sample-to-sample fluctuations. However, the similarity between the results, in each single run and on the average, substantiates our method, and yields a reliable estimate for the correlation length.

B. Hg spreading on Au (gold) films

The spreading process of Hg droplets on thin *gold* films [28] differs from the silver case by two major aspects: (i) The chemical reaction between the droplet and the surface, which plays a major role in the dynamics of the interface, is extremely different [28]; (ii) the roughness of the surfaces, gold and silver, prior to the Hg deposition is different. In order to estimate quantitatively the structure of the surfaces, atomic force microscope (AFM) measurements were carried out. They show that both surfaces have a pinned-shape structure. However, while the average pin height of the silver surface is 200 Å and its average pin width (at the half height) is 1000 Å, the corresponding results for the gold surface are 100 Å (height) and 500 Å (width), namely, the gold surface structure is different.

Therefore the Hg-Au system can be considered as a totally different system. Moreover, the values obtained for both scaling exponents, α and β, which were found to be much

higher comparing to the silver systems [28], attribute this system to a different category as well. Similarly to Figs. 5, 8, and 9, we show in Fig. 10 data of mercury droplet that spreads on a thin gold film. The value of β was found to be $\beta=0.76$ with a standard deviation of 0.03 between similar experiments. The correlation length, L_α, obtained by the crossover behavior of the roughness exponent (α) was found to be 45 pixels (7 μm) whereas the corresponding length scale observed in the $\Delta \log W$ vs L graph, L_β, was found to be 54 pixels (8.5 μm). Therefore we conclude that our method yields a reasonably well estimate for the correlation length in this similar, but different, system.

V. IMBIBITION PROCESS

How general is our approach? As mentioned above, apart from the recent experiments by Balankin *et al.* [21] and Soriano *et al.* [22], there are very few plots of the function $W(t)$ in the literature [15–19]. These experiments have been performed for a wide spectrum of growing interfaces, such as growth of thin metal layers by vacuum evaporation [15–17], magnetic domain-wall roughening in alloy films [18] and imbibition of water on paper [19]. Most of these experimental results are for single interfaces. The corresponding log-log plots have been fitted to a growth exponent β, while ignoring the fluctuations that *did* appear in all of them, in various magnitudes. This neglect can sometimes be justified, as the magnitude of the fluctuations, determined by the parameters λ and ν in the relevant KPZ equation, can be small (see Fig. 6).

In Ref. [19], Family *et al.* have made an imbibition experiment with water spreading on paper. In their Fig. 2, they show the growing interface in a sequence of 11 different times from 450 s up to 7200 s (2 h). We have analyzed their data in order to obtain the growth and roughness exponents, and calculated both $W(t)$ and $W(L)$ from their data (Fig. 11). We have found that indeed, $W(t)$ exhibits the expected nonmonotonic behavior [Fig. 11(a)]. Moreover, the correlation length emerging from the plot of $\Delta \log W$ vs L [Fig. 11(b)] is similar to the length scale emerging from the crossover in $W(L)$ [Fig. 11(c)]. This length scale is about 18 pixels (9 mm). Their $W(t)$ plot for another single experiment, with another type of paper (their Fig. 4), also exhibits the same nonmonotonic behavior discussed above. The time and length scales of this experiment differ by a few orders of magnitude from our spreading experiments described above. Thus, it confirms that our method can be applied to a wide range of length and time scales.

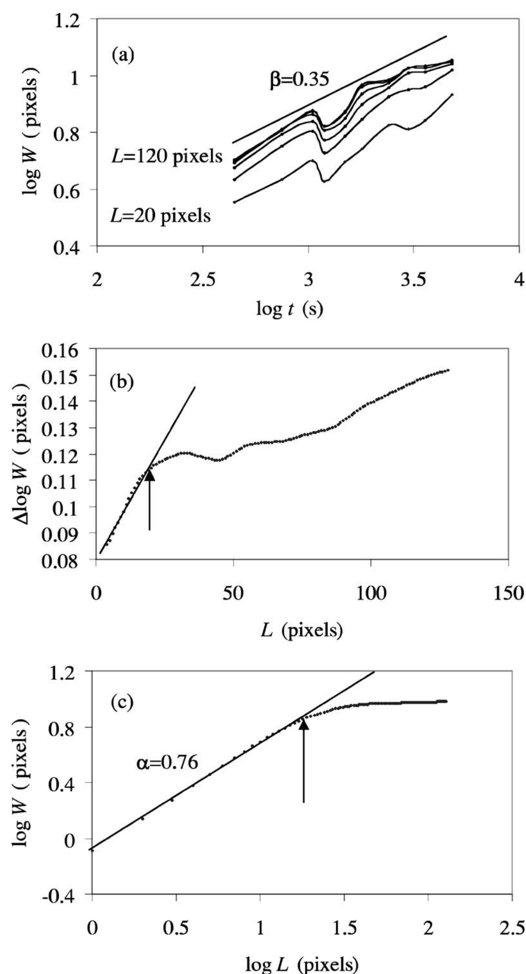

FIG. 11. (a) The function $W(t)$ calculated from the data in Fig. 2 of Family *et al.* [19], for window sizes L varying from 20 to 120 pixels, which are about 10 to 60 mm. The nonmonotonic function is riding over the straight line (slope of about 0.35). (b) The fluctuation measure $\Delta \log W$ as a function of the window size L. A crossover is marked with an arrow for $L=18$ pixels (9 mm). (c) The roughness exponent α, calculated from the upper interface (7200 s) in Fig. 2 of [19]. A crossover is marked with an arrow for the same length scale $L=18$ pixels (9 mm) as in (b). The roughness exponent was found to be $\alpha=0.76$ below the crossover.

VI. SUMMARY

In summary, we have investigated the special features of single kinetic roughening processes. The width growth function $W(t)$ for a single interface exhibits temporal fluctuations which result from the competition between normal growth and surface tension forces. This claim was verified using numerical solutions of the QKPZ equation for a wide range of its parameters. We have shown that the size of the fluctuations contains important information, which allows one to obtain a characteristic length in the system. We have presented a method to extract this length from the data and showed that it is valid for a wide range of systems, ranging from very small scales (mercury spreading on thin silver and gold films) up to large scales (water spreading on paper). We are currently studying the fluctuations and the correlation length as a function of the metal film surface roughness.

ACKNOWLEDGMENTS

This research was supported by The Israel Science Foundation (Grant No. 1342/04). We thank Yael Hoss for technical assistance.

[1] A. L. Barabasi and H. E. Stanley, *Fractal Concepts in Surface Growth* (Cambridge University Press, Cambridge, UK, 1995).
[2] A. Bunde and S. Havlin, *Fractals and Disordered Systems*, 2nd ed. (Springer-Verlag, Berlin, 1996).
[3] A. Bunde and S. Havlin, *Fractals in Science*, 2nd ed. (Springer-Verlag, Berlin, 1994).
[4] P. Meakin, *Fractals, Scaling, and Growth Far from Equilibrium* (Cambridge University Press, Cambridge, UK, 1998).
[5] T. Vicsek, *Fractal Growth Phenomena*, 2nd ed. (World Scientific, Singapore, 1992).
[6] M. Alava, M. Dube, and M. Rost, Adv. Phys. **53**, 83 (2004), and references cited therein.
[7] M. Kardar, G. Parisi, and Y. C. Zhang, Phys. Rev. Lett. **56**, 889 (1986).
[8] H. G. E. Hentschel and F. Family, Phys. Rev. Lett. **66**, 1982 (1991).
[9] J. M. Lopez, Phys. Rev. E **52**, R1296 (1995).
[10] M. H. Jensen and I. Procaccia, J. Phys. II **1**, 1139 (1991).
[11] J. Yang and G. Hu, Phys. Rev. E **55**, 1525 (1997).
[12] V. K. Horvath, F. Family, and T. Vicsek, J. Phys. A **24**, L25 (1991).
[13] V. K. Horvath and H. E. Stanley, Phys. Rev. E **52**, 5166 (1995).
[14] L. N. Paritskaya, V. V. Bogdanov, Yu. S. Kaganovskii, W. Lojkowski, D. Kolesnikov, and A. Presz, Defect Diffus. Forum **194–199**, 1539 (2001).
[15] H. You, R. P. Chiarello, H. K. Kim, and K. G. Vandervoort, Phys. Rev. Lett. **70**, 2900 (1993).
[16] H. J. Ernst, F. Fabre, R. Folkerts, and J. Lapujoulade, Phys. Rev. Lett. **72**, 112 (1994).
[17] C. Thompson, G. Palasantzas, Y. P. Feng, S. K. Sinha, and J. Krim, Phys. Rev. B **49**, 4902 (1994).
[18] M. Jost, J. Heimel, and T. Kleinefeld, Phys. Rev. B **57**, 5316 (1998).
[19] F. Family, K. C. B. Chan, and J. G. Amar, in *Surface Disordering: Growth, Roughening and Phase Transition*, edited by R. Jullien, J. Kertesz, P. Meakin, and D. E. Wolf (Nova Science, New York, 1992), pp. 205–211.
[20] J. Maunuksela, M. Myllys, O. P. Kahkonen, J. Timonen, N. Provatas, M. J. Alava, and T. Ala-Nissila, Phys. Rev. Lett. **79**, 1515 (1997).
[21] A. S. Balankin, A. Bravo-Ortega, and D. M. Matamoros, Philos. Mag. Lett. **80**, 503 (2000).
[22] J. Soriano, J. Ortin, and A. Hernandez-Machado, Phys. Rev. E **66**, 031603 (2002).
[23] S. V. Buldyrev, A. L. Barabasi, F. Caserta, S. Havlin, H. E. Stanley, and T. Vicsek, Phys. Rev. A **45**, R8313 (1992).
[24] T. Sun, H. Guo, and M. Grant, Phys. Rev. A **40**, R6763 (1989).
[25] P. Meakin and R. Jullien, Phys. Rev. A **41**, 983 (1990).
[26] A. Be'er, Y. Lereah, and H. Taitelbaum, Physica A **285**, 156 (2000).
[27] A. Be'er, Y. Lereah, I. Hecht, and H. Taitelbaum, Physica A **302**, 297 (2001).
[28] A. Be'er, Y. Lereah, A. Frydman, and H. Taitelbaum, Physica A **314**, 325 (2002).
[29] P. G. de Gennes, Rev. Mod. Phys. **57**, 827 (1985).
[30] A. M. Cazabat, Contemp. Phys. **28**, 347 (1987).
[31] L. Leger and J. F. Joanny, Rep. Prog. Phys. **55**, 431 (1992).
[32] A. Be'er and Y. Lereah, J. Microsc. **208**, 148 (2002).
[33] M. J. de Ruijter, J. De Coninck, and G. Oshanin, Langmuir **15**, 2209 (1999).
[34] J. Leopoldes, A. Dupuis, D. G. Bucknall, and J. M. Yeomans, Langmuir **19**, 9818 (2003).
[35] F. G. Yost, F. M. Hosking, and D. R. Frear, *The Mechanics of Solder-Alloy Wetting and Spreading* (Van Nostrand Reinhold, New York, 1993).
[36] Y. M. Liu and T. H. Chuang, J. Electron. Mater. **29**, 405 (2000).
[37] H. T. Hayslett, Jr., *Statistics Made Simple*, 1st ed. (Doubleday and Company Inc., Garden City, NY, 1968).
[38] C. K. Peng, S. V. Buldyrev, A. L. Goldberger, S. Havlin, F. Sciortino, M. Simons, and H. E. Stanley, Nature (London) **356**, 168 (1992).
[39] C. K. Peng, S. Havlin, H. E. Stanley, and A. L. Goldberger, Chaos **5**, 82 (1995).
[40] H. Press, S. A. Teukolsky, W. T. Vetterling, and B. P. Flannery, *Numerical Recipes in C* (Cambridge University Press, Cambridge, UK, 1992).